Equilibrium Conditions for Semi-Clathrate Hydrates Formed with CO_2, N_2 or CH_4 in the Presence of Tri-n-butylphosphine Oxide

Jianwei Du and Liguang Wang *
School of Chemical Engineering, The University of Queensland, Brisbane, QLD 4072, Australia.

ABSTRACT We measured the thermodynamic stability conditions for the N_2, CO_2, or CH_4 semi-clathrate hydrate formed from the aqueous solution of Tri-n-butylphosphine Oxide (TBPO) at 26 wt%, corresponding to the stoichiometric composition for TBPO·34.5H_2O. The measurements were performed at the temperature range of (283.71 to 300.34) K and pressure range of (0.35 to 19.43) MPa with using an isochoric equilibrium step-heating pressure search method. The results showed that the presence of TBPO made these semi-clathrate hydrates much more stable than the corresponding pure N_2, CO_2, and CH_4 hydrates. At a given temperature, the semi-clathrate hydrate of 26 wt% TBPO solution + CH_4 was more stable than that of 26 wt% TBPO solution + CO_2, which in turn was more stable than 26 wt% TBPO solution + N_2. We analyzed the phase equilibrium data using the Clausius-Clapeyron equation and found that at the pressure range of (0 to 20) MPa, the mean dissociation enthalpies for the semi-clathrate hydrates systems of 26 wt% TBPO solution + N_2, 26 wt% TBPO solution + CO_2, and 26 wt% TBPO solution + CH_4 were 177.75 kJ·mol^{-1}, 206.23 kJ·mol^{-1} and 159.00 kJ·mol^{-1}, respectively.

Keywords: Carbon dioxide hydrate, Nitrogen hydrate, Methane hydrate, Semi-clathrate hydrate, Tri-n-butylphosphine oxide, Phase equilibria, Dissociation enthalpy

1. INTRODUCTION

Gas hydrates are a group of ice-like crystalline compounds stabilized under low temperature and elevated pressure conditions.[1] Accommodating guest molecules of certain size by gas hydrates has found its potential applications in gas storage and separation.[2, 3] However, the high pressure requirement and slow formation kinetics remain an impediment to the technology development for hydrate-based gas separation, storage, and transport.

One of the promising methods for reducing the pressure requirement for hydrate formation is to use chemical additives, which can lead to the formation of semi-clathrate hydrates (SCHs) at relatively high temperatures and low pressures. SCHs were first reported by Fowler et al.[4] in 1940 and were subsequently analyzed using X-ray diffraction by McMullan and Jeffrey [5]. The latter found that in some clathrate hydrates, the guest molecules such as organic salts not only occupy the voids, but also act as part of the cages. These SCH crystalline solids are built up by the water-anion-framework containing empty dodecahedral cavities and large cavities encaging the cations covalently bonded to alkyl chains. Shimada et al. [6] provided the first evidence that unoccupied cages in SCH could enclathrate suitably sized gas molecules, such as hydrogen sulphide, methane and nitrogen, and suggested that the SCH could be used for separating gas molecules. Kamata et al. [7] then experimentally showed that with tetra-n-butyl ammonium bromide (TBAB) as a SCH former, it was possible to separate smaller molecules (e.g. nitrogen, methane, and hydrogen sulfide) from larger molecules (e.g. ethane, propane and carbon dioxide). In other words, SCHs are capable of selectively incorporating small gas guest molecules within the small cavities of the SCHs. Unlike ordinary hydrates having well defined structures (Structure I, Structure II, and Structure H), SCHs have diverse structures and have hydrogen-bonding interaction between guests and hosts molecules, which is much stronger than the van

der Waals force in ordinary hydrates[5]

SCHs have drawn increasingly more interest from researchers for their potential applications in hydrogen storage [8], carbon dioxide storage [9], and gas separation [10-14]. The thermodynamic data of SCHs are limited, and the majority of them are for TBAB [8, 15-32]. More phase equilibrium data on SCHs are needed for acquiring in-depth knowledge of gas hydrate formation, optimizing the thermodynamic models, and developing effective gas processing technologies.

One of the SCH formers, which are less known, is tri-n-butylphosphine oxide (TBPO). TBPO and water could form both TBPO·28H_2O and TBPO·34.5H_2O SCHs under atmospheric pressure, with the melting point being 279.65 and 280.25 K, respectively [33, 34]. The latter TBPO hydrate with higher melting point has a crystal unit composed of four $5^{12}6^4$ cages, four $5^{12}6^3$ cages, four $5^{12}6^2$ cages, and fourteen 5^{12} cages associated with 138 H_2O in real structure[33], and the empty 5^{12} cage can encage small gas molecules. Recently, Gholinezhad [12] reported one phase equilibrium data point (i.e. 280.25 K, 0.1 MPa) of CH_4 with TBPO solution at a stoichiometric concentration (26 wt%). To the best of our knowledge, there are no other studies on SCHs formed in the systems of gas + TBPO + water. In the present study, we systematically report the phase equilibrium data for the SCHS with N_2, CH_4 or CO_2 + 26 wt % TBPO solution.

2. EXPERIMENTAL

2.1. Materials

TBAB (0.99 mass fraction pure) and TBPO (0.95 mass fraction pure) used in this work were supplied by Sigma-Aldrich. CH_4 (0.99995 volume fraction pure), N_2 (0.99999 volume fraction pure) and CO_2 (0.99995 volume fraction pure) were obtained from Coregas. All of these materials were used as received. Deionized water was used to prepare the aqueous solutions of TBPO or TBAB.

2.2. Experimental apparatus

A schematic diagram and specifications of the experimental apparatus are given in Figure 1. The high pressure reactor used in the present work was a home-made non-visual 102 ml stainless steel cylindrical vessel with inside diameter of 38 mm and inside depth of 90 mm. The reactor was immersed in a liquid bath, which was connected to a temperature control circulator (PC200-A25, Thermo Scientific) with temperature stability of 0.01 K. The bath was covered by two heat insulation layers to ensure that the constant-temperature step could be controlled precisely at 0.1 K. A thermowell coupled with a matched 1/10 DIN ultra precise immersion RTD sensor (Omega) was inserted into ¾ depth of the reactor to measure the liquid or hydrate phase temperature with an uncertainty of ± 0.03 K. A pressure transducer (OMEGA) with accuracy of ± 0.01 MPa (± 0.03% and pressure range of 34.5 MPa) was used to measure the gas pressure inside the reactor. A magnetically driven stirrer (PTFE-coated cross bar, purchased from Industrial Equipment and Control) was used to agitate the test liquid. The gas discharged from the gas booster (Maximator MGB-ROB8-37) was fed into the reactor. The experimental data were collected at 10 seconds intervals using a data acquisition system (Agilent 34970A).

2.3. Experimental procedure

The high pressure cell was cleaned at least seven times with using deionized water and dried prior to the introduction of TBAB or TBPO aqueous solution. The cell was filled with 30 g of 26 wt% TBPO solution, corresponding to the stoichiometric ratio TBPO·34.5H_2O. Likewise, TBAB solutions (30 g) were prepared for examining the reliability of the current experimental system. Finally, the test solution was loaded into the clean and dry reactor. A vacuum pump (Javac CC-45) was used to degas the entire system except the reactor for 5 to 10 minutes. Subsequently, the test solution in the reactor was degassed for 0.5 - 1 minute before

undergoing hydrate experiments. The effect of degassing on the concentration of the test solution was negligible.

The hydrate phase equilibrium measurements were performed at the temperature range of (283.71 to 300.34) K and pressure range of (0.35 to 19.43) MPa with using an isochoric equilibrium step-heating pressure search method[1]. Figure 2 shows typical pressure-temperature traces for the SCHs obtained in the present work. For each experimental run, the temperature was initially set at 303 K, and the initial gas pressure was set at a specific value (e.g. 20, 15, 10, 6, or 2 MPa). The temperature in the reactor was gradually reduced at a rate of 0.5 K per hour with a 1-hour constant-temperature stage after every 5-hour temperature decreasing until 273.2 K, while the rotating speed of the magnetic stirrer remained high at around 600 rpm (corresponding to Reynolds number ~7000) to obtain an adequate mixing. A sudden drop of gas pressure indicated the onset of the hydrate formation, and the hydrate formation ended at around 274 K. The duration of hydrate formation process took about 1 to 2 days, depending on the initial pressure. The temperature was then increased first at a relatively large rate of 0.2 K per hour, which is considered acceptable for reducing the time requirement.[35] After every five-hour continuous heating, there was a one-hour constant-temperature stage. Once the temperature was close to (usually 1-2 K lower than) the possible dissociation point which can be inferred from the pressure-temperature trace, the stepwise heating rate was adjusted to 0.1 K for every 6 hours. Between these temperature rising stages were two-hour constant-temperature stages. The hydrate dissociation point was determined from the abrupt change in the slope of the hydrate dissociation line approaching the initial cooling line. As shown in Figure 2a, the typical pressure-temperature trace of TBAB + N_2 hydrate is similar to those reported in the literature.[25,36] For TPBO + N_2 hydrate, however, Figure 2b shows an unusual pressure-temperature trace. Similar pressure-temperature traces were obtained for TPBO + CO_2 hydrate and

TPBO + CH_4 hydrate. This abnormal increase in pressure near the end of hydrate formation suggests that with TPBO, a pronounced change in crystal structure might have occurred. The release of gas at lower temperature could be explained by two different gas hydrate phases (e.g. gas-containing hydrate and gas-free hydrate) in equilibrium with a peritectic liquid. Note that there are at least two structures for TBPO hydrate: TBPO·34.5H_2O and TBPO·28H_2O.[33] Further work with using spectroscopic techniques is under way to understand this phenomenon.

3. RESULTS AND DISCUSSION

First, the reliability and accuracy of the apparatus and isochoric experimental procedure was verified by comparing the phase equilibrium data of TBAB + water + N_2 and TBAB + water + CH_4 obtained in the present work with the corresponding data in the literature. Next, we reported the phase equilibrium data for SCHs with 26 wt% TBPO solution + N_2, CO_2, or CH_4. Finally, we estimated the dissociation enthalpies of these TBPO-containing SCHs.

3.1 Examination of the reliability of the current experimental system

The phase equilibrium data for 5 wt% TBAB solution + N_2 semi-clathrate hydrate were shown in Table 1 and Figure 3. Also plotted in Figure 3 are the data reported by Lee et al. [19], Mohanmmadi et al. [25] and Duc et al. [9] using the same method. As shown in Figure 3, the data obtained in the present work are in good agreement with those reported in refs [19,25], and these three sets of data fall essentially on the same line. The role of thermal path, especially the heating rate and heating paths (continuous and stepwise), in determining the accuracy of gas hydrate phase equilibrium data using isochoric method has been discussed in detail by Tohidi et al.[35] and Mohammad et al.[36]

The repeatability of our experimental data can be seen from Figure 1S and Table 1S in Support Information.

We have repeated the measurement twice for one hydrate dissociation point of 5 wt% TBAB solution + N_2. The standard deviation of measured temperature was 0.03 K, and the standard deviation of measured pressure was 0.01 MPa, within the uncertainty range of the RTD and pressure transducer used in the present work.

The phase equilibrium data for 10 wt% TBAB solution + CH_4 semi-clathrate hydrate are shown in Table 2 and Figure 4. Also plotted in Figure 4 are the data reported by Refs [8, 21, 25]. Again, these three sets of data fall essentially on the same line, indicating that our experimental setup applying the equilibrium step-heating pressure-search method is reliable over the pressure range under study.

3.2 Experimental phase equilibrium data of 26 wt% TBPO solution + N_2, CH_4 or CO_2 hydrates

We measured the phase equilibrium conditions for SCHs with 26 wt% TBPO solution + N_2, 26 wt% TBPO solution + CO_2, and 26 wt% TBPO solution + CH_4, and the results are shown in Figure 5 and Table 3. The systems exhibit three-phase equilibrium: SCH phase + aqueous phase + vapor phase. In Figure 5, the upper left region of each curve represents the conditions at which the solid SCH phase (H) is stable for the relevant system and in the lower right region, the solid SCH phase (H) disappears and only aqueous phase (Lw) and vapor phase (V) are present. As shown, the equilibrium pressure steadily decreased with decreasing temperature. All these curves which represent different guest gases appear to converge at a certain point where the temperature was approximately 284 K. At a temperature above 284 K, however, the SCH of 26 wt% TBPO solution + CH_4 was considerably more stable than that of 26 wt% TBPO solution + CO_2, which in turn was much more stable than that of 26 wt% TBPO + N_2. Note that the curve of 26 wt% TBPO solution + CH_4 is below that of 26 wt% TBPO solution + CO_2. By contrast, the phase equilibrium curve of pure CH_4 hydrate is above that of pure CO_2 hydrate at the temperature range under study.

Figure 6 compares the phase equilibrium data obtained in the present work for 26 wt% TBPO solution

(corresponding to TBPO·34.5H_2O[33]) with those from the literature[25] for the SCHs of 25 wt% TBAB aqueous solution, with CO_2, N_2 or CH_4. Note that in the literature[25] the equilibrium data with 26 wt% TBAB are not available, and the closest is 25 wt%. Also plotted in the sub-figures are the pure gas hydrate equilibrium data[25]. As shown, the presence of TBPO made these SCHs much more stable than the corresponding pure CO_2, N_2 and CH_4 hydrates, with the equilibrium pressure being dropped by approximately 10- to 100-fold at 285 K. The effect of TBPO on reducing the phase equilibrium pressure was comparable with that of TBAB except the CO_2 hydrate, for which TBAB gave slightly milder hydrate equilibrium conditions than TBPO.

Figure 7 compares the effects of TBPO and TBAB on the hydrate phase equilibrium conditions. Note that in the presence of TBAB, the semi-clathrate hydrate phase equilibrium curves of CO_2 and CH_4 are close to each other and even have a crossover. By contrast, with TBPO, the SCH phase equilibrium curves of CO_2 and CH_4 are far from each other and more importantly, there is no crossover between these two phase equilibrium curves. These results provide a clue that TBPO could potentially be more useful than TBAB for gas separation applications, including removal of CO_2 from conventional natural gas and purification of coal seam gas (coal bed methane). Further work is under way to investigate the potential of TBPO for gas separation, including selectivity and efficiency.

TBPO is a very strong hydrogen-bond acceptor, while TBAB is a strong proton acceptor. The difference in the molecular structure between TBPO and TBAB should have a significant impact on the intermolecular interactions and thus the enthalpies during the process of CO_2 hydrate formation and dissociation. In what follows, we analyzed the phase equilibrium data using the Clausius-Clapeyron equation to roughly estimate the dissociation enthalpies of these SCHs.

3.3. Dissociation enthalpy of 26 wt% TBPO + N_2, CH_4 or CO_2 hydrates

The dissociation enthalpies ($\Delta_{dis}H_m$) of the semi-clathrate hydrates were determined by using a modified Clausius-Clapeyron equation:[40, 41]

$$\frac{d\ln P}{d(1/T)} = -\frac{\Delta_{dis}H_m}{zR} \quad (1)$$

where R is the gas constant and z is the compressibility factor that accounts for the non-ideality of the gases. The z values were calculated using the SRK equation of state, which is highly accurate for N_2, CH_4 and CO_2 at non-ideality. These z values are shown in Table 2S. Equation (1) is a simplification of the Clapeyron equation. Here, only the gas phase is considered and the dissolved gas is neglected. For CO_2, Equation (1) could also be applicable in spite of the relatively high solubility of CO_2 in water, and the calculated $\Delta_{dis}H_m$ values are in good agreement with those reported in the literatures.[42-44]

Figure 8 shows the semilogarithmic plots of hydrate dissociation pressure versus reciprocal absolute temperature ($\ln P$ versus $1/T$), and the straight lines represent the best linear fit of the experimental data. As shown, for N_2 and CH_4, the slopes of the lines for TBPO semiclathrate hydrates were larger than those of TBAB, whereas for CO_2, the slope for TBPO semiclathrate hydrate was smaller than that of TBAB. In using Equation (1), the value of $d\ln P/d(1/T)$ was set equal to the slope of the fitted straight lines shown in Figure 8. The mean enthalpies of dissociation for the 26 wt% TBPO solution + N_2, CO_2 and CH_4 systems and the 25 wt% TBAB aqueous solution + N_2, CO_2 and CH_4 system were shown in Table 4 along with those of the corresponding pure gas hydrates. Note that the $\Delta_{dis}H_m$ values were largely determined by the slope of $\ln P$ versus $1/T$. As shown, with these different guest gas molecules, TBPO gave the CO_2 semi-clathrate hydrate the highest dissociation enthalpy, whereas TBAB gave the CO_2 semi-clathrate hydrate the lowest. The changes in the $\Delta_{dis}H_m$ of SCHs with TBPO follow the same trend as the pure gas hydrates. This difference

suggests that TBPO and TBAB should differ greatly in getting involved with the hydrate formation through cavity occupation and hydrogen bonding interaction. It has been accepted that the Br^+ ions dissociated from TBAB in water can play a role in forming the cages in the SCHs, whereas no such anions but phosphoryl oxygen from TBPO can get involved with the cage formation. These arguments and conjectures point to the need for more work to understand the observed difference in the pressure - temperature trace between TBAB and TBPO (see Figure 2), especially near the end of hydrate formation and the start of hydrate dissociation.

It is known that the enthalpy of dissociation is determined by the cavity sizes occupied by the guests for ordinary hydrate such as sI and sII; the size of hydrate guest increases in the order of N_2, CH_4, and CO_2, so is the slope of the fitted straight lines for the ln$P$ versus 1/T plots.[1] For SCHs, however, there is no apparent relationship between the fitted straight lines for the ln$P$ versus 1/T plots and the sizes of cavities or SCH formers. SCH formers participate in the cage structure or framework mainly through hydrogen bonding, in contrast to ordinary hydrate guest molecules that are incorporated into the hydrate cage mainly through van der Waals force. Furthermore, the hydrogen bonding interaction is much stronger than van der Waals force, so the interaction between the SCH formers and water molecular of SCHs cages should be quite different from that between the guest molecular and water molecular in ordinary cages. As can be seen from Table 4, the $\Delta_{dis}H_m$ values of the SCHs are systematically larger than the corresponding pure gas hydrates.

4. SUMMARY AND CONCLUSIONS

A 102-ml stirred reactor was used to measure the phase equilibrium conditions for SCHs using the isochoric equilibrium step-heating pressure search method. The reliability and accuracy of the apparatus and isochoric experimental procedure was verified by comparing the phase equilibrium data of 5 wt% TBAB solution + N_2 and 10 wt% TBAB solution + CH_4 obtained in the present work with the corresponding data in

the literature.

The phase equilibrium conditions of 26 wt% TBPO solution and CO_2, N_2 or CH_4 semi-clathrate hydrates were measured in the temperature range of (283.71 to 300.34) K and pressure range of (0.35 to 19.43) MPa. It was found that addition of TBPO allowed the dissociation conditions of the CO_2, N_2 or CH_4 hydrate to shift to higher temperatures and lower pressures. Over the temperature range of (283.7 to 300.3) K, the semi-clathrate hydrate of 26 wt% TBPO solution + CH_4 was substantially more stable than that of 26 wt% TBPO solution + CO_2, which in turn was more stable than 26 wt% TBPO solution + N_2.

We estimated the dissociation enthalpies of these TBPO-containing SCHs. The dissociation enthalpies were calculated from the measured phase equilibrium data of the N_2, CH_4 or CO_2 + 26 wt% TBPO solution semi-clathrate hydrates using the Clausius-Clapeyron equation. The mean dissociation enthalpies for the N_2, CH_4 or CO_2 + 26 wt% TBPO solution semi-clathrate hydrates systems at the pressure range of (0 to 20) MPa were 177.75 $kJ \cdot mol^{-1}$, 206.23 $kJ \cdot mol^{-1}$ and 159 $kJ \cdot mol^{-1}$, respectively.

ASSOCIATED CONTENT

Supporting Information. Reproducibility of experimental data (Figure 1s and Table 1s); compressibility factor and dissociation enthalpy (Table 2s). This material is available free of charge via the Internet at http://pubs.acs.org.

AUTHOR INFORMATION

Corresponding Author

*Tel: +61-7-33657942; E-mail: L.Wang2@uq.edu.au.

ACKNOWLEDGEMENTS

The authors gratefully appreciate the financial support from Australian Research Council under the

Discovery Projects scheme (No. 1092846) and thank Mr. Douglas Malcolm for designing the high pressure reactor.

REFERENCES

1. Sloan, E. D.; Koh, C. A., *Clathrate Hydrates of Natural Gases, Third Edition*. CRC Press, Taylor & Francis: New York, 2008.

2. Happel, J.; Hnatow, M. A.; Meyer, H., The study of separation of nitrogen from methane by hydrate formation using a novel apparatus. In *International Conference on Natural Gas Hydrates*, New York Acad Sciences: New York, 1994; 715, 412-424.

3. Rossi, F.; Filipponi, M.; Castellani, B., Investigation on a novel reactor for gas hydrate production. *Appl. Energ.* **2012,** 99, 167-172.

4. Fowler, D. L.; Loebenstein, W. V.; Pall, D. B.; Kraus, C. A., Some Unusual Hydrates of Quaternary Ammonium Salts. *J. Am. Chem. Soc.* **1940,** 62, (5), 1140-1142.

5. McMullan, R.; Jeffrey, G. A., Hydrates of the Tetra n-butyl and Tetra i-amyl Quaternary Ammonium Salts. *J. chem. phys.* **1959,** 31, (5), 1231-1234.

6. Shimada, W.; Ebinuma, T.; Oyama, H.; Kamata, Y.; Takeya, S.; Uchida, T.; Nagao, J.; Narita, H., Separation of gas molecule using tetra-n-butyl ammonium bromide semi-clathrate hydrate crystals. *Jpn. J. Appl. Phys.2* **2003,** 42, (2A), 129-131.

7. Kamata, Y.; Oyama, H.; Shimada, W.; Ebinuma, T.; Takeya, S.; Uchida, T.; Nagao, J.; Narita, H., Gas separation method using tetra-n-butyl ammonium bromide semi-clathrate hydrate. *Jpn. J. Appl. Phys.1* **2004,** 43, (1), 362-365.

8. Arjmandi, M.; Chapoy, A.; Tohidi, B., Equilibrium data of hydrogen, methane, nitrogen, carbon dioxide,

and natural gas in semi-clathrate hydrates of tetrabutyl ammonium bromide. *J. Chem. Eng. Data* **2007,** 52, (6), 2153-2158.

9. Duc, N. H.; Chauvy, F.; Herri, J.-M., CO_2 capture by hydrate crystallization – A potential solution for gas emission of steelmaking industry. *Energ. Convers. Manage.* **2007,** 48, (4), 1313-1322.

10. Fan, S.; Li, S.; Wang, J.; Lang, X.; Wang, Y., Efficient capture of CO_2 from simulated flue gas by formation of TBAB or TBAF semiclathrate hydrates. *Energ. Fuel.* **2009,** 23, (8), 4202-4208.

11. Li, S.; Fan, S.; Wang, J.; Lang, X.; Wang, Y., Clathrate Hydrate Capture of CO_2 from Simulated Flue Gas with Cyclopentane/Water Emulsion. *Chinese J. Chem. Eng.* **2010,** 18, (2), 202-206.

12. Gholinezhad, J. Experimental investigation of semi-clathrate hydrates with application towards gas storage, transportation and separation. PhD Dissertation, Heriot-Watt University, 2012.

13. Ricaurte, M.; Dicharry, C.; Broseta, D.; Renaud, X.; Torre, J. P., CO_2 Removal from a CO_2-CH_4 Gas Mixture by Clathrate Hydrate Formation Using THF and SDS as Water-Soluble Hydrate Promoters. *Ind. Eng. Chem. Res.* **2013,** 52, (2), 899-910.

14. Zhong, D. l.; Ye, Y.; Yang, C.; Bian, Y.; Ding, K., Experimental Investigation of Methane Separation from Low-Concentration Coal Mine Gas (CH_4/N_2/O_2) by Tetra-n-butyl Ammonium Bromide Semiclathrate Hydrate Crystallization. *Ind. Eng. Chem. Res.* **2012,** 51, (45), 14806-14813.

15. Deschamps, J.; Dalmazzone, D., Dissociation enthalpies and phase equilibrium for TBAB semi-clathrate hydrates of N_2, CO_2, N_2+ CO_2 and CH_4+ CO_2. *J. Therm. Anal. Calorim.* **2009,** 98, (1), 113-118.

16. Li, X. S.; Xia, Z. M.; Chen, Z. Y.; Yan, K. F.; Li, G.; Wu, H.-J., Equilibrium hydrate formation conditions for the mixtures of CO_2+ H_2+ tetrabutyl ammonium bromide. *J. Chem. Eng. Data* **2009,** 55, (6), 2180-2184.

17. Makino, T.; Yamamoto, T.; Nagata, K.; Sakamoto, H.; Hashimoto, S.; Sugahara, T.; Ohgaki, K.,

Thermodynamic stabilities of tetra-n-butyl ammonium chloride + H_2, N_2, CH_4, CO_2, or C_2H_6 semiclathrate hydrate systems. *J. Chem. Eng. Data* **2009,** 55, (2), 839-841.

18. Mohammadi, A. H.; Richon, D., Phase equilibria of semi-clathrate hydrates of tetra-n-butylammonium bromide + hydrogen sulfide and tetra-n-butylammonium bromide+ methane. *J. Chem. Eng. Data* **2009,** 55, (2), 982-984.

19. Lee, S.; Lee, Y.; Park, S.; Seo, Y., Phase Equilibria of Semiclathrate Hydrate for Nitrogen in the Presence of Tetra-n-butylammonium Bromide and Fluoride. *J. Chem. Eng. Data* **2010,** 55, (12), 5883-5886.

20. Mohammadi, A. H.; Richon, D., Phase equilibria of semi-clathrate hydrates of tetra-n-butylammonium bromide + hydrogen sulfide and tetra-n-butylammonium bromide + methane. *J. Chem. Eng. Data* **2010,** 55, (2), 982-984.

21. Sun, Z. G.; Sun, L., Equilibrium conditions of semi-clathrate hydrate dissociation for methane + tetra-n-butyl ammonium bromide. *J. Chem. Eng. Data* **2010,** 55, (9), 3538-3541.

22. Bouchafaa, W.; Dalmazzone, D.; et Procédés, U. C., Thermodynamic equilibrium data for mixed hydrates of CO_2–N_2, CO_2–CH_4 and CO_2–H_2 in pure water and TBAB solutions, Proceedings of the 7th International Conference on Gas Hydrates, Edinburgh, UK, 2011; 2011.

23. Hughes, T. J.; Marsh, K. N., Methane Semi-Clathrate Hydrate Phase Equilibria with Tetraisopentylammonium Fluoride. *J. Chem. Eng. Data* **2011,** 56, (12), 4597-4603.

24. Mayoufi, N.; Dalmazzone, D.; Delahaye, A.; Clain, P.; Fournaison, L.; Fürst, W., Experimental Data on Phase Behavior of Simple Tetrabutylphosphonium Bromide (TBPB) and Mixed CO_2 + TBPB Semiclathrate Hydrates. *J. Chem. Eng. Data* **2011,** 56, (6), 2987-2993.

25. Mohammadi, A. H.; Eslamimanesh, A.; Belandria, V.; Richon, D., Phase equilibria of semiclathrate

hydrates of CO_2, N_2, CH_4, or H_2+ Tetra-n-butylammonium bromide aqueous solution. *J. Chem. Eng. Data* **2011,** 56, (10), 3855-3865.

26. Tumba, K.; Reddy, P.; Naidoo, P.; Ramjugernath, D.; Eslamimanesh, A.; Mohammadi, A. H.; Richon, D., Phase Equilibria of Methane and Carbon Dioxide Clathrate Hydrates in the Presence of Aqueous Solutions of Tributylmethylphosphonium Methylsulfate Ionic Liquid. *J. Chem. Eng. Data* **2011,** 56, (9), 3620-3629.

27. Jin, Y.; Kida, M.; Nagao, J., Phase Equilibrium Conditions for Clathrate Hydrates of Tetra-n-butylammonium Bromide (TBAB) and Xenon. *J. Chem. Eng. Data* **2012,** 57, (6), 1829-1833.

28. Sun, Z. G.; Liu, C. G., Equilibrium Conditions of Methane in Semiclathrate Hydrates of Tetra-n-butylammonium Chloride. *J. Chem. Eng. Data* **2012,** 57, (3), 978-981.

29. Yang, H.; Fan, S.; Lang, X.; Wang, Y.; Sun, X., Hydrate Dissociation Conditions for Mixtures of Air + Tetrahydrofuran, Air + Cyclopentane, and Air + Tetra-n-butyl Ammonium Bromide. *J. Chem. Eng. Data* **2012,** 57, (4), 1226-1230.

30. Lin, W.; Dalmazzone, D.; Fürst, W.; Delahaye, A.; Fournaison, L.; Clain, P., Thermodynamic Studies of CO_2 + TBAB + Water System: Experimental Measurements and Correlations. *J. Chem. Eng. Data* **2013**.

31. Shi, L. L.; Liang, D. Q.; Li, D. L., Phase Equilibrium Data of Tetrabutylphosphonium Bromide Plus Carbon Dioxide or Nitrogen Semiclathrate Hydrates. *J. Chem. Eng. Data* **2013,** 58, (7), 2125-2130.

32. Suginaka, T.; Sakamoto, H.; Iino, K.; Sakakibara, Y.; Ohmura, R., Phase equilibrium for ionic semiclathrate hydrate formed with CO_2, CH_4, or N_2 plus tetrabutylphosphonium bromide. *Fluid Phase Equilibr.* **2013,** 344, (0), 108-111.

33. Alekseev, V. I.; Gatilov, Y. V.; Polyanskaya, T. M.; Bakakin, V. V.; Dyadin, Y. A.; Gaponenko, L. A., Characteristic features of the production of the hydrate framework around the hydrophobic-hydrophilic unit in

the crystal structure of the clathrate tri-n-butylphosphine oxide 34.5-hydrate. *J. Struct. Chem.* **1982,** 23, (3), 395-399.

34. Dyadin, Y. A.; Udachin, K., Clathrate polyhydrates of peralkylonium salts and their analogs. *J. Struct. Chem.* **1987,** 28, (3), 394-432.

35. Tohidi, B.; Burgass, R.; Danesh, A.; Østergaard, K.; Todd, A., Improving the accuracy of gas hydrate dissociation point measurements. *Ann. NY. Acad. Sci.* **2000,** 912, (1), 924-931.

36. Mohammad-Taheri, M.; Zarringhalam Moghaddam, A.; Nazari, K.; Gholipour Zanjani, N., The role of thermal path on the accuracy of gas hydrate phase equilibrium data using isochoric method. *Fluid Phase Equilibr.* **2013,** 338, (0), 257-264.

37. Mohammadi, A. H.; Tohidi, B.; Burgass, R. W., Equilibrium data and thermodynamic modeling of nitrogen, oxygen, and air clathrate hydrates. *J. Chem. Eng. Data* **2003,** 48, (3), 612-616.

38. Mooijer-van den Heuvel, M. M.; Witteman, R.; Peters, C. J., Phase behaviour of gas hydrates of carbon dioxide in the presence of tetrahydropyran, cyclobutanone, cyclohexane and methylcyclohexane. *Fluid Phase Equilibr.* **2001,** 182, (1–2), 97-110.

39. Servio, P.; Englezos, P., Measurement of Dissolved Methane in Water in Equilibrium with Its Hydrate. *J. Chem. Eng. Data* **2001,** 47, (1), 87-90.

40. Van der Waals, J.; Platteeuw, J., Clathrate solutions. *Adv. Chem. Phys.* **1959,** 2, (1), 1-57.

41. Sloan, E.; Fleyfel, F., Hydrate dissociation enthalpy and guest size. *Fluid Phase Equilibr.* **1992,** 76, 123-140.

42. Kwon, T. H.; Kneafsey, T. J.; Rees, E. V. L., Thermal Dissociation Behavior and Dissociation Enthalpies of Methane-Carbon Dioxide Mixed Hydrates. *J. Phys. Chem. B* **2011,** 115, (25), 8169-8175.

43. Mayoufi, N.; Dalmazzone, D.; Fürst, W.; Elghoul, L.; Seguatni, A.; Delahaye, A.; Fournaison, L., Phase behaviour of tri-n-butylmethylammonium chloride hydrates in the presence of carbon dioxide. *J. Therm. Anal. Calorim.* **2012,** 109, (1), 481-486.

44. Sabil, K. M.; Witkamp, G.-J.; Peters, C. J., Estimations of enthalpies of dissociation of simple and mixed carbon dioxide hydrates from phase equilibrium data. *Fluid Phase Equilibr.* **2010,** 290, (1-2), 109-114.

Figure captions

Figure. 1. Schematic of the experimental apparatus used for phase equilibrium measurements (not drawn to scale).

Figure. 2. Determination of hydrate dissociation point from typical pressure-temperature traces obtained in the present work: a), 5 wt% TBAB aqueous solution + N_2; b), 26 wt% TBPO aqueous solution + N_2.

Figure 3. Phase equilibrium data for TBAB + H_2O + N_2 semi-clathrate hydrate at 5 wt%: ●, this work (isochoric equilibrium step-heating pressure-search method); □, ref 19 (the same method); △, ref 25 (the same method). The dashed line represents the best fit of the experimental data obtained in the present work.

Figure 4. Phase equilibrium data for 10 wt% TBAB + CH_4 semi-clathrate hydrate: ●, this work (isochoric equilibrium step-heating pressure-search method); □, ref 17 (the same method); ∆, ref 21 (the same method); ○, ref 22 (the same method).

Figure 5. Experimental phase equilibrium data for three systems: ■ (black), 26 wt% TBPO + N_2; ● (red), 26 wt% TBPO + CO_2; ▲ (green), 26 wt% TBPO + CH_4.

Figure 6. Comparison of experimental phase equilibrium data for various hydrate systems.

Figure 7. Experimental phase equilibrium data: ● (red), 26 wt% TBPO aqueous solution + CO_2, this work; ▲ (green), 26 wt% TBPO aqueous solution + CH_4, this work; ○ (red), 25 wt% TBAB aqueous solution + CO_2, ref 25. △ (green), 25 wt% TBAB aqueous solution + CH_4, ref 25.

Figure 8. Semilogarithmic plot of semi-clathrate hydrate phase equilibrium pressure versus reciprocal phase equilibrium temperature: systems with 26 wt% TBPO aqueous solution + (a) N_2, (c) CO_2, and (e) CH_4, in the present work; systems with 25 wt% TBAB aqueous solution + (b) N_2, (d) CO_2, and (f) CH_4, from ref 25.

Table 1. Semi-clathrate Hydrate Phase Equilibrium Data of 5 wt% TBAB aqueous solution + N_2,

T/K	*P*/MPa
287.31	19.12
287.09	18.33
286.63	16.07
285.88	13.99
285.11	11.64
284.67	10.31
284.14	9.01
283.63	7.76
282.51	5.62
280.95	3.92

Table 2. Phase equilibrium data for 10 wt% TBAB + CH_4 semi-clathrate hydrate

T/K	P/MPa
291.47	8.55
289.4	4.69
286.96	2.33

Table 3. Semi-clathrate Hydrate Phase Equilibrium Data in the Three Component Systems of TBPO + H_2O + N_2, CO_2 and CH_4, Corresponding to the Boundary Condition between Water-Hydrate-Vapor (Lw + H + V) Phases and Water-Vapor (Lw + V) Phases.

Phase	*T*/K	*P*/MPa
	26 wt% TBPO + N_2	
	284.12	1.02
	285.14	2.03
	286.88	3.71
	287.82	4.83
	289.01	6.15
	289.97	7.54
	290.93	8.94
	291.89	10.79
	292.31	11.83
	292.94	13.44
	293.14	13.96
	293.63	15.18
	294.04	17.17
	294.49	19.43
	26 wt% TBPO + CO_2	
Lw +H+V > Lw +V	283.94	0.56
	285.27	0.85
	286.62	1.51
	287.94	2.57
	289.79	3.81
	26 wt% TBPO + CH_4	
	283.71	0.35
	287.21	0.79
	289.72	1.44
	292.06	2.17
	292.93	2.96
	293.67	3.69
	294.31	4.34
	296.04	6.86
	297.47	10.14
	298.58	12.98
	299.66	15.63
	300.34	18.9

Table 4. Enthalpies of dissociation $\Delta_{dis}H_m$/kJ·mol^{-1} for N_2, CO_2 and CH_4 in 25 wt% TBAB solution, 26 wt% TBPO solution and pure water

Guest	TBPO	TBAB[a]	Pure water[b]
N_2	177.75	319.04	62.98
CO_2	206.23	195.03	70.03
CH_4	159.00	265.18	59.39

[a] Calculations made on the basis of phase equilibrium data source of ref 25

[b] Calculations made on the basis of phase equilibrium data source of ref 37-39

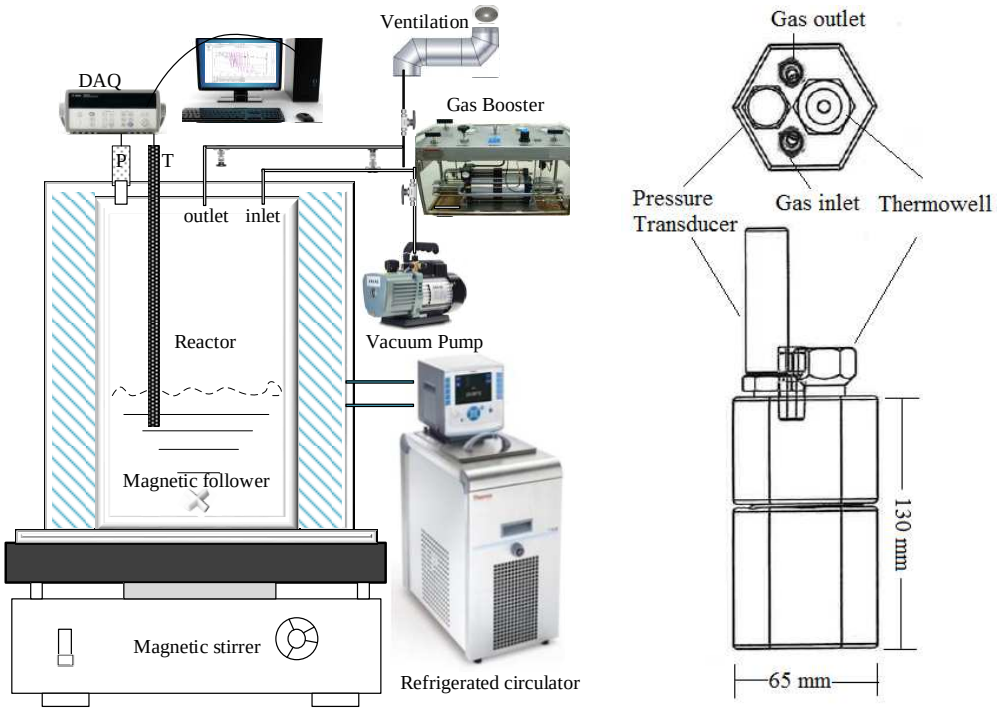

(a), phase equilibrium measurement system (b), the high pressure reactor

Figure 1. Schematic of the experimental apparatus used for phase equilibrium measurements (not drawn to scale).

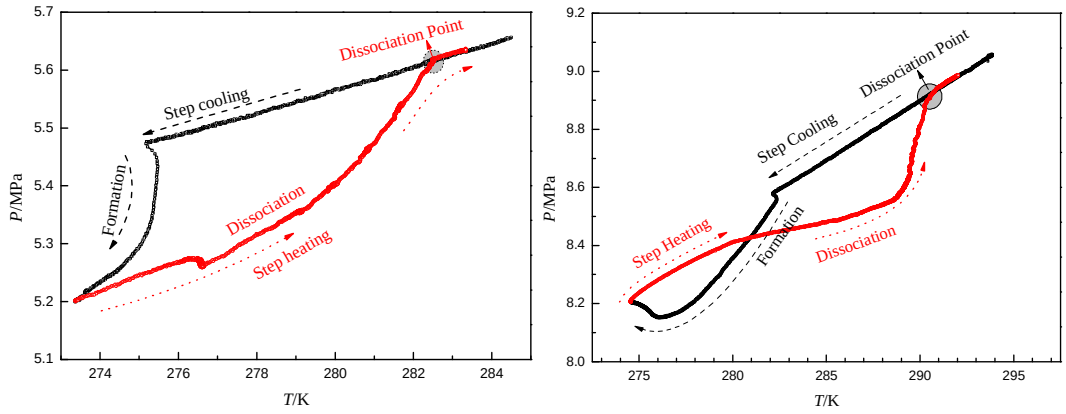

Figure 2. Determination of hydrate dissociation point from typical pressure-temperature traces obtained in the present work: a), 5 wt% TBAB aqueous solution + N_2; b), 26 wt% TBPO aqueous solution + N_2.

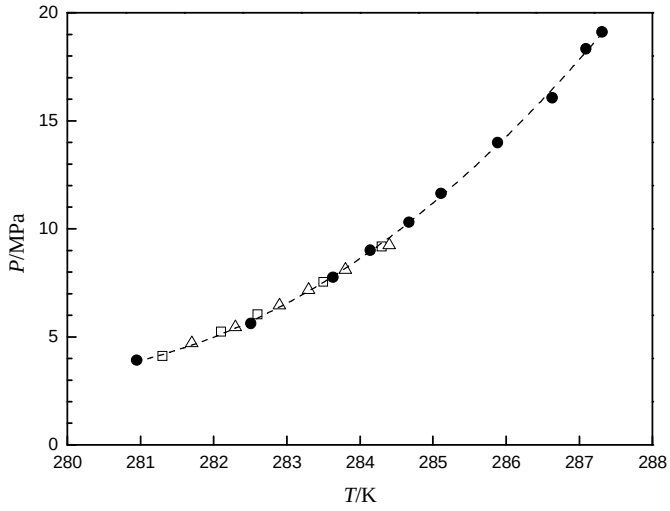

Figure 3. Phase equilibrium data for 5 wt% TBAB + N_2 semi-clathrate hydrate: ●, this work (isochoric equilibrium step-heating pressure-search method); □, ref 19 (the same method); △, ref 25 (the same method). The dashed line represents the best fit of the experimental data obtained in the present work.

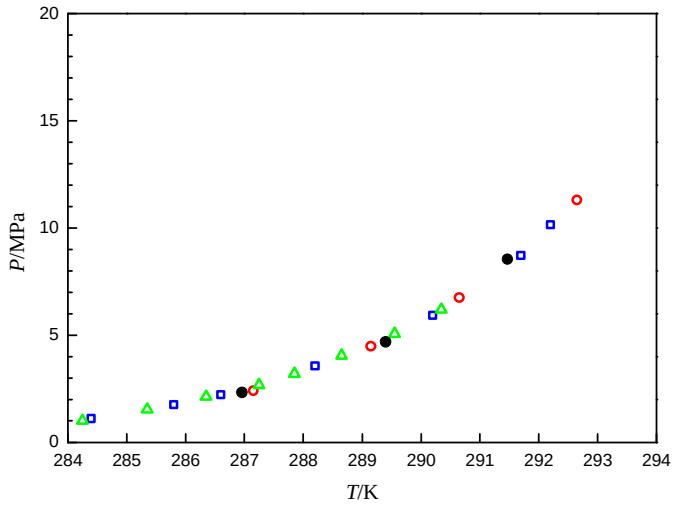

Figure 4. Phase equilibrium data for 10 wt% TBAB + CH_4 semi-clathrate hydrate: ●, this work (isochoric equilibrium step-heating pressure-search method); □, ref 17 (the same method); △, ref 21 (the same method); ○, ref 22 (the same method).

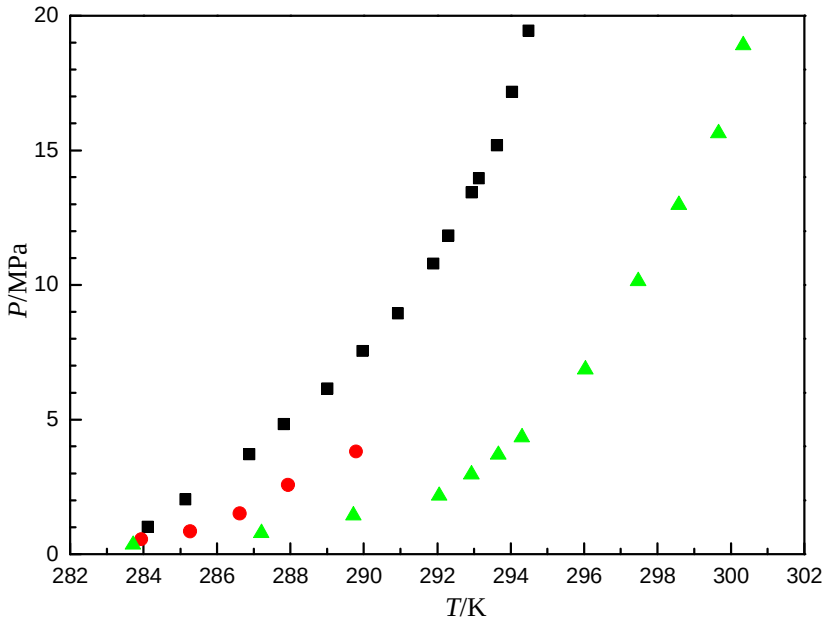

Figure 5. Experimental phase equilibrium data for three systems: ■ (black), 26 wt% TBPO + N_2; ● (red), 26 wt% TBPO + CO_2; ▲ (green), 26 wt% TBPO + CH_4.

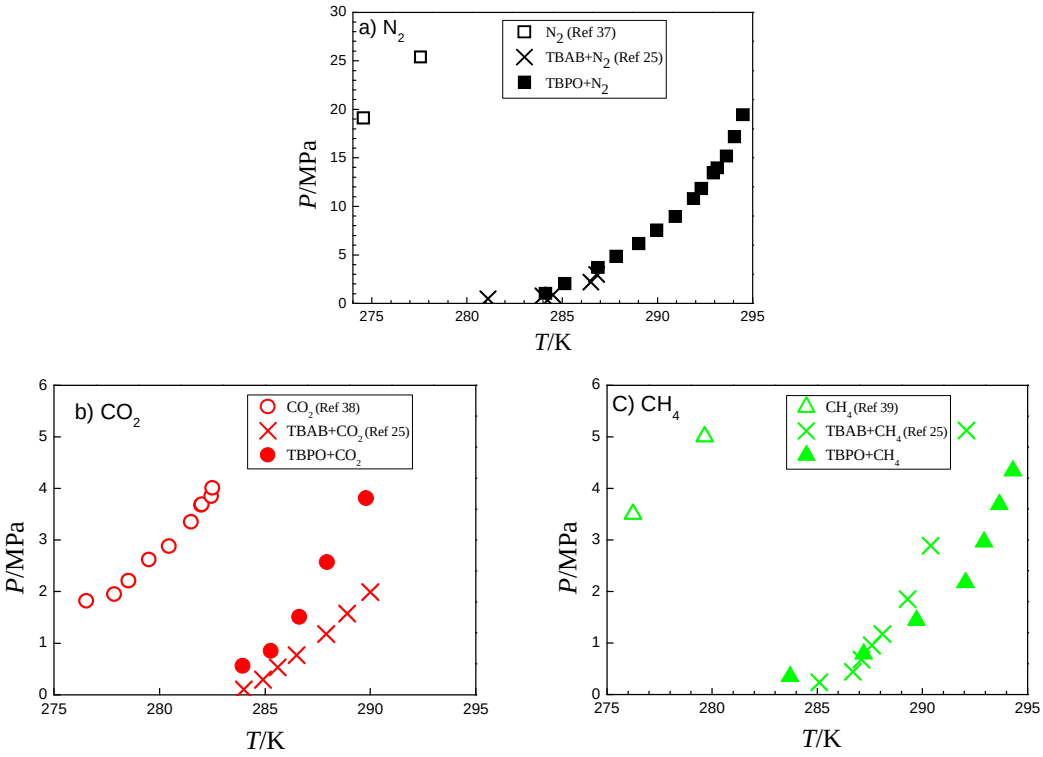

Figure 6. Comparison of experimental phase equilibrium data for various hydrate systems.

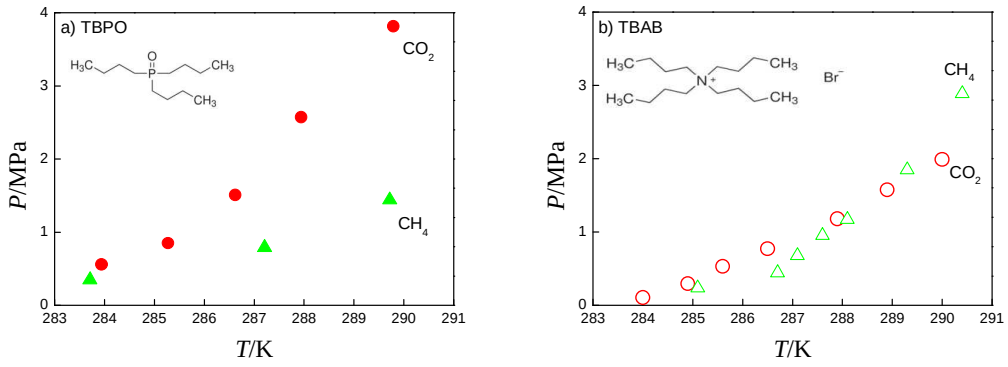

Figure 7. Experimental phase equilibrium data: ● (red), 26 wt% TBPO aqueous solution + CO_2, this work; ▲ (green), 26 wt% TBPO aqueous solution + CH_4, this work; ○ (red), 25 wt% TBAB aqueous solution + CO_2, ref 25. △ (green), 25 wt% TBAB aqueous solution + CH_4, ref 25.

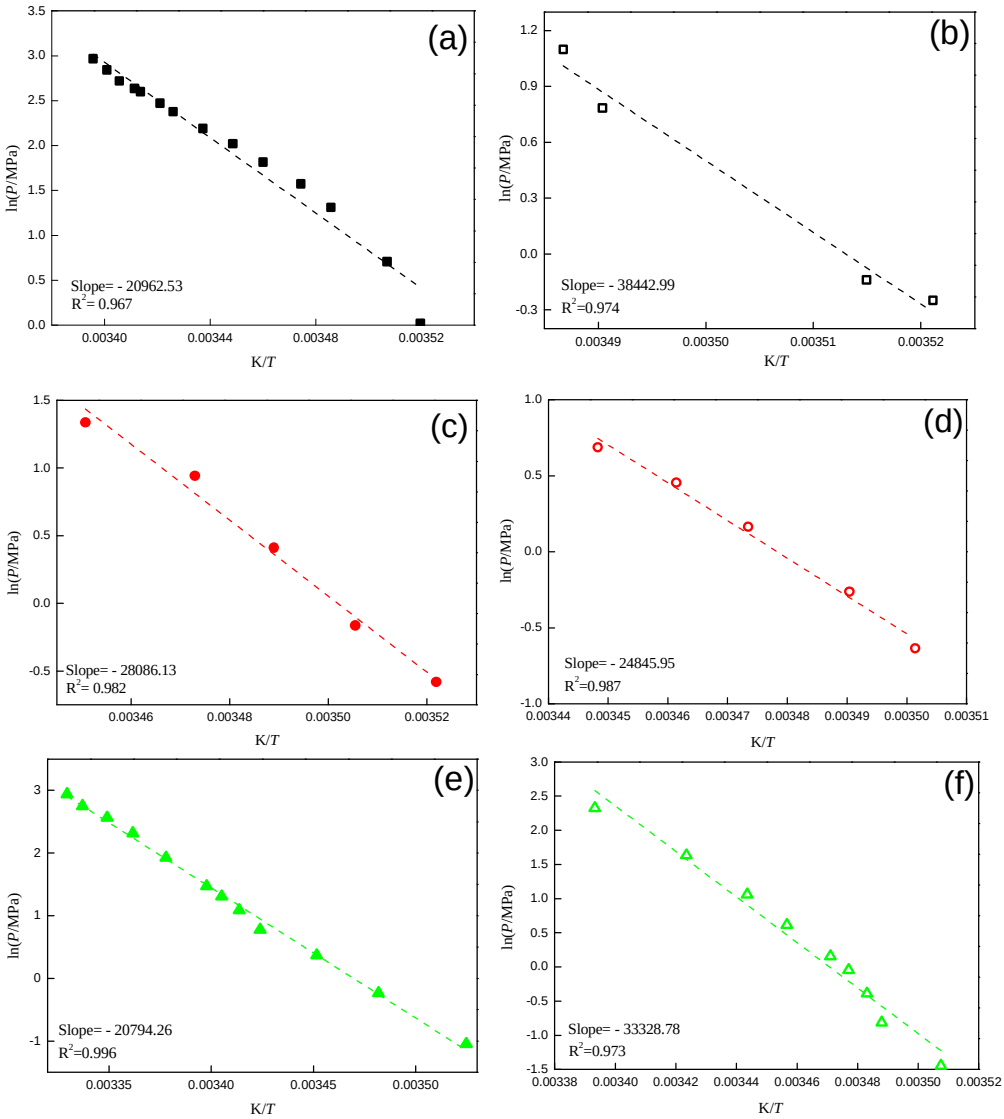

Figure 8. Semilogarithmic plot of semi-clathrate hydrate phase equilibrium pressure versus reciprocal phase equilibrium temperature: systems with 26 wt% TBPO aqueous solution + (a) N_2, (c) CO_2, and (e) CH_4, in the present work; systems with 25 wt% TBAB aqueous solution + (b) N_2, (d) CO_2, and (f) CH_4, from ref 25.

for Table of Contents use only